Available online at www.sciencedirect.com
ScienceDirect
Journal of Molecular Catalysis A: Chemical 259 (2006) 302–308
JOURNAL OF MOLECULAR CATALYSIS A: CHEMICAL
www.elsevier.com/locate/molcata

Effect of the *cis*- and *trans*-[1,2-bis(diphenylphosphino)ethylene] ligands in the properties of diphosphine–polypyridyl complexes of ruthenium(II) Application to electrocatalytic oxidations of organic compounds

Eliana M. Sussuchi, Andréia A. de Lima, Wagner F. De Giovani *

Departamento de Química, Faculdade de Filosofia, Ciências e Letras de Ribeirão Preto, Universidade de São Paulo, Av. Bandeirantes 3900, 14040-901 Ribeirão Preto, São Paulo, Brazil

Received 11 January 2006; received in revised form 24 May 2006; accepted 25 May 2006
Available online 30 August 2006

Abstract

The ruthenium(II) complexes [Ru(*cis*-L)(totpy)(H_2O)](PF_6)$_2$ (**1**) and [Ru(*trans*-L)$_2$(totpy)(H_2O)](PF_6)$_2$ (**2**) (L = 1,2-bis(diphenylphosphino)ethylene; totpy = 4′-(4-tolyl)-2,2′:6′,2″-terpyridine) were synthesized and characterized by elemental analysis, cyclic and differential pulse voltammetries and UV–vis, IR and ^{31}P NMR spectra. The redox potentials of **2** are less anodic than those of **1**. The redox potentials are a result of the different environments created by the phosphine ligands in the *trans*-complex, associated with their electron donating effect. Electrocatalytic oxidations of benzyl alcohol, cyclohexanol, 1-pentanol, 1,2-butanediol, 1,4-butanediol and cyclohexene were performed using complexes **1** and **2** both in solution and immobilized in carbon paste electrode.

Keywords: Ruthenium aquacomplexes; Phosphine ligands; Polypyridyl ligands; Carbon paste electrodes; Electrocatalytic oxidation

1. Introduction

In recent years, many ruthenium complexes have been prepared and characterized for application in electrocatalysis, photolysis, bioinorganic chemistry, asymmetrical catalytic hydrogenation, among other fields [1–9].

New synthetic procedures for the obtention of terpyridine- and bipyridine-substituted ligands have been developed to improve the performance and the chelating ability of the ligands, resulting in adequate changes in the electrochemisty and spectroscopic states of transition metal complexes containing these ligands [10,11]. The electrochemical behaviour of ruthenium(II)–polypyridyl complexes has been intensely investigated [4–9,12–14].

Aqua polypyridyl complexes are an important class of compounds, and their electrochemical oxidation can produce high oxidation states in ruthenium complexes containing oxo ligands, which are exceptionally reactive sites for multi-electronic oxidation of substrates [4–19]. The high interest in the redox chemistry of ruthenium oxo complexes is partly due to the stabilization of the high oxidation states easily achieved by the metal (IV–VI) in processes involving rapid proton transfer concomitant with electron transfer [6,20]. Oxo ruthenium complexes are known to be useful stoichiometric and electrocatalytic oxidants for the transformation of a variety of inorganic and organic substrates [4–10,15].

The potential catalytic activity of ruthenium(II) complexes containing chiral diphosphine ligands has been previously described [3,13,14].

In this work, we describe the syntheses of [Ru(*cis*-L)(totpy)(H_2O)](PF_6)$_2$ (**1**) and [Ru(*trans*-L)$_2$(totpy)(H_2O)](PF_6)$_2$ (**2**) (L = 1,2-bis(diphenylphosphino)ethylene; totpy = 4′-(4-tolyl)-2,2′:6′,2″-terpyridine), as well as their spectral, electrochemical, and catalytic properties. We aimed at investigating how a bulky donating group in the 4′-position of terpyridine could influence the chelating properties of this well-known ligand. Whereas the *cis*-diphosphine ligand leads to a chelating coordination mode, the *trans*-diphosphine ligand is a non-chelating species due to the rigid double bond. The ability of the complexes to act as catalysts in the electro-oxidation of organic compounds was studied in both homogeneous solution and immobilized in carbon paste electrode.

* Corresponding author. Tel.: +55 16 3602 3810; fax: +55 16 3602 4838.
E-mail address: wfdgiova@usp.br (W.F. De Giovani).

1381-1169/$ – see front matter © 2006 Elsevier B.V. All rights reserved.
doi:10.1016/j.molcata.2006.05.059

2. Experimental

2.1. Materials

Water was doubly distilled from alkaline potassium permanganate. $RuCl_3 \cdot xH_2O$, *cis*- and *trans*-1,2-bis(diphenylphosphino)ethylene were purchased from Aldrich Chemical Co. Methylene chloride and acetonitrile were kept in an alumina column before being used. All other reagents and solvents were used without further purification.

2.2. Instrumentation and measurements

Routine UV–vis spectra were obtained in 1 cm quartz cells by using a Hewlett-Packard 8453 spectrophotometer. Electrochemical experiments were carried out in a PAR model 273A Potentiostat/Galvanostat. $E_{1/2}$ values for reversible couples were calculated from half the difference between E_p values for the cathodic and anodic waves. Cyclic voltammetric and differential pulse voltammetric experiments were performed in a one-compartment cell using a glassy carbon working electrode, a platinum wire auxiliary electrode, and a saturated calomel (SCE) or Ag/AgCl reference electrode. Bulky electrolyses were performed in 7:3 phosphate buffer:*tert*-butyl alcohol solutions, in a 50 mL two-compartment cylindrical cell, using a platinum gauze working electrode (164 cm^2), a platinum plate auxiliary electrode (1 cm^2), and an SCE. Electrolyses were carried out at $25 \pm 1\,^{\circ}C$, at fixed applied potentials of +1.18 and +1.10 V when **1** and **2** were used as catalysts, respectively. The potential applied in each case was sufficient to generate $Ru^{IV}=O^{2+}$ oxidizing species from the corresponding Ru^{II}–OH_2^{2+} complexes. Electrolyses were allowed to continue until the current fell to residual values or until the desired number of coloumbs was reached. The electrolyses products were extracted with diethyl ether and analyzed by gas chromatography (GC); the chromatograms were recorded in an Intralab 3000 gas chromatograph. The pH values of aqueous solutions were buffered at an ionic strength of 0.25 mol L^{-1} by using HNO_3 and $NaNO_3$ (pH 2.0), potassium hydrogen phthalate, HNO_3 and $NaNO_3$ (pH 3.0), potassium hydrogen phthalate, NaOH and $NaNO_3$ (pH 4.0–5.5), Na_2HPO_4 and NaH_2PO_4 (pH 6.0–8.0), $Na_2B_4O_7 \cdot 10H_2O$ and $NaNO_3$ (pH 9.0), $Na_2B_4O_7 \cdot 10H_2O$ and NaOH (pH 10.0–10.8). Elemental analyses were performed using a CHNS-O CE Instruments model EA 1110 elemental analyzer. Ruthenium analyses were performed in a V-85 B Braun ICP-AES atomic emission spectrometer. EPR spectra of the solid complexes were recorded at room temperature on a Bruker EP 200D spectrometer. ^1H NMR and ^{31}P NMR spectra were obtained in a Brucker AC-300 spectrometer. Mass spectra were obtained in a Hewlett-Packard gas chromatograph/MS system 5988A.

2.3. Preparation of the ligand 4′-(4-tolyl)-2,2′:6′,2″-terpyridine (totpy)

The ligand 4′-(4-tolyl)-2,2′:6′,2″-terpyridine was prepared analogously to a literature procedure [14]. A 2:1 ratio of 2-acetylpyridine:*p*-tolualdehyde was used. The solid was recrystallized from ethanol and were obtained light green crystals (54% yield) identified as 4′-(4-tolyl)-2,2′:6′,2″-terpyridine (totpy). ^1H NMR: m, 8.65–8.85 ($H_{3,3''}$; $H_{6,6''}$; $H_{3',5'}$); m, 7.80–8.00 ($2H_o$; $H_{4,4''}$); m, 7.35–7.45 ($2H_m$; $H_{5,5''}$); s, 2.47 (–CH_3). EI MS: *m/z* 323.20. Anal. calc. for $C_{22}H_{17}N_3$: C 81.71%; H 5.30%; N 12.99%. Found: C 82.09%; H 5.28%; N 13.38%.

2.4. Synthesis of the complexes

$[RuCl_3(totpy)]$ was prepared according to a procedure reported in the literature [21,22] (85% yield).

2.4.1. [Ru(cis-L)(totpy)Cl]Cl

A mixture of $[RuCl_3(totpy)]$ (0.20 g, 0.38 mmol) and *cis*-1,2-bis(diphenylphosphino)ethylene (0.18 g, 0.45 mmol) was heated to reflux, under N_2 atmosphere, in 60 mL of a 3:1 dichloroethane:ethanol solution, in the presence of NEt_3 (0.25 mL) and LiCl (0.08 g, 1.89 mmol), for 3.0 h. The hot solution was filtered and its volume was evaporated to dryness. The product was recrystallized by dissolving it in acetone and precipitating by addition of diethyl ether. Yield: 0.27 g (80%).

2.4.2. [Ru(trans-L)$_2$(totpy)Cl](PF$_6$)

This complex was prepared using a procedure similar to that employed for the obtention of [Ru(*cis*-L)(totpy)Cl]Cl. The difference was that a 2:1:1 ethanol:ethylene glycol:water ratio and a two-fold quantity (0.36 g, 0.90 mmol) of *trans*-L ligand were used. The hot solution was filtered and 2.0 mL of an NH_4PF_6 saturated aqueous solution were added to the filtrate. Red brown crystals were obtained. Yield: 0.32 g (60%).

2.4.3. [Ru(cis-L)(totpy)(H$_2$O)](PF$_6$)$_2$ (**1**)

[Ru(*cis*-L)(totpy)Cl]Cl (0.10 g; 0.11 mmol) and silver *p*-toluenesulfonate (0.08 mg; 0.26 mmol) were heated to reflux in 40 mL of 1:1 ethanol:water, under N_2 atmosphere, for 5 h. The hot solution was filtered and 2.0 mL of an NH_4PF_6 saturated aqueous solution were added to the filtrate. The volume was reduced to 20 mL in a rotary evaporator. The brown crystals were collected by filtration, washed with cold water and diethyl ether, and dried under vacuum. The complex was reprecipitated from acetone–diethyl ether. Yield: 0.08 g (65%).

2.4.4. [Ru(trans-L)$_2$(totpy)(H$_2$O)](PF$_6$)$_2$ (**2**)

This complex was prepared using a procedure similar to that employed for the obtention of **1**. The difference was that the solution was refluxed for 1.5 h under N_2 atmosphere. Yield: 0.11 g (69%).

2.5. Modified electrodes

2.5.1. Carbon paste electrodes

Carbon paste electrodes [8,23] containing 3:22 by weight of complex:paste were used for cyclic voltammetric studies. The paste was prepared by mixing 3:2 by weight of carbon powder:mineral oil. The carbon paste holder consisted of a thick-walled Teflon tube with 0.3 cm i.d. A copper sleeve equipped with a copper wire plunger was mounted at the top of the Teflon

Table 1
Elemental analysis and ^{31}P NMR data for the complexes

Complexes	^{31}P NMR δ (ppm)[a]	Calc./exp.		
		C (%)	H (%)	Ru (%)
[Ru(totpy)Cl_3]	–	49.82/48.95	3.23/3.28	–
[Ru(*cis*-L)(totpy)Cl]Cl	69.5 (d), 63.5 (d)	64.64/63.70	4.41/4.12	–
[Ru(*trans*-L)$_2$(totpy)Cl](PF_6)	152.2 (s)	63.59/65.20	4.39/4.15	–
[Ru(*cis*-L)(totpy)(H_2O)](PF_6)$_2$ (**1**)	73.5 (d), 65.7 (d)	51.07/51.91	3.66/3.97	8.95/9.20
[Ru(*trans*-L)$_2$(totpy)(H_2O)](PF_6)$_2$ (**2**)	153.4 (s)	58.27/56.56	4.16/4.07	6.63/6.85

[a] CH_2Cl_2 (H_3PO_4/85%).

tube. By rotating the sleeve, it was possible to make the plunger extrude an used past layer which was sliced off to form a fresh paste surface.

3. Results and discussion

3.1. Synthesis

The reaction between [$RuCl_3$(totpy)] and the diphosphine ligands (*cis*- and *trans*-$Ph_2PCH{=}CHPPh_2$), produced distinct complexes. The product containing *cis*-1,2-bis(diphenylphosphino)ethylene favors the chelating coordination mode, so compound [Ru(*cis*-L)(totpy)Cl]Cl is preferentially formed. However, in the case of the *trans*-$Ph_2PCH{=}CHPPh_2$ ligand, which is non-chelating [24–26] due to its rigid backbone, the dominant product was [Ru(*trans*-L)$_2$(totpy)Cl](PF_6). The chloride species are converted in good yield to the corresponding aqua complexes, by using Ag(I) ion under reflux in ethanol/water. Elemental analysis data are shown in Table 1.

3.2. EPR and ^{31}P NMR spectroscopies

The ^{31}P NMR spectrum of **1** displays a double doublet of similar intensity in the 73.5–65.7 ppm range (Fig. 1a), showing that the phosphorus atoms are not equivalent. On the other hand, the spectrum of complex **2** displays only a single singlet at 153.4 ppm (Fig. 1b), indicating that all phosphorus atoms are equivalent and that the two ligands are in *trans*-position. The ^{31}P NMR data are summarized in Table 1 and correspond to the structures shown in Fig. 2.

EPR spectra of ruthenium(III) complexes give *g* tensor values [27] that can be used to derive ground states. The **1** and **2** aqua complexes show no EPR signals, indicating the oxidation state Ru(II).

3.3. Electronic absorption spectra

The spectral data are summarized in Table 2. The intense bands in the UV region are assignable to ligands $\pi \rightarrow \pi^*$ transitions. The band in the visible region, at $\lambda_{max} = 418$ nm for **1** can be attributed to metal–ligand dπ (Ru) $\rightarrow \pi^*$ (totpy) transitions; the wide band at $\lambda_{max} = 475$ nm for **2** can be attributed to metal–ligand dπ (Ru) $\rightarrow \pi^*$ (diphosphine) transitions and it also contains the metal–ligand dπ (Ru) $\rightarrow \pi^*$ (totpy) transitions [12]. The transitions of the *trans*-complex are of lower energy than those of *cis*-complex. This fact can be attributed to the effect of the two phosphine ligands in *trans*. In this case, when π-acceptor ligands such as phosphines find themselves in *trans*-positions to each other, they compete for the electrons of the metallic center with the same intensity, leaving it rich in electronic density. Such competition favors a high delocalization of the electronic density in the metal in favor of the π-acceptor phosphine ligands, explaining the lower energy of the MLCT transition of complex **2**.

Both aqua complexes have similar spectra. As observed in the case of other aqua complexes, the MLCT energy shifts to higher values upon substitution of the anionic chloride ligand for the neutral aqua ligand [8,10].

The correlation between MLCT energies of various complexes and their respective electrochemical redox potentials ($E_{1/2}$) has been reported [7a]. It has been observed that complexes with lower transition energies have lower redox potentials.

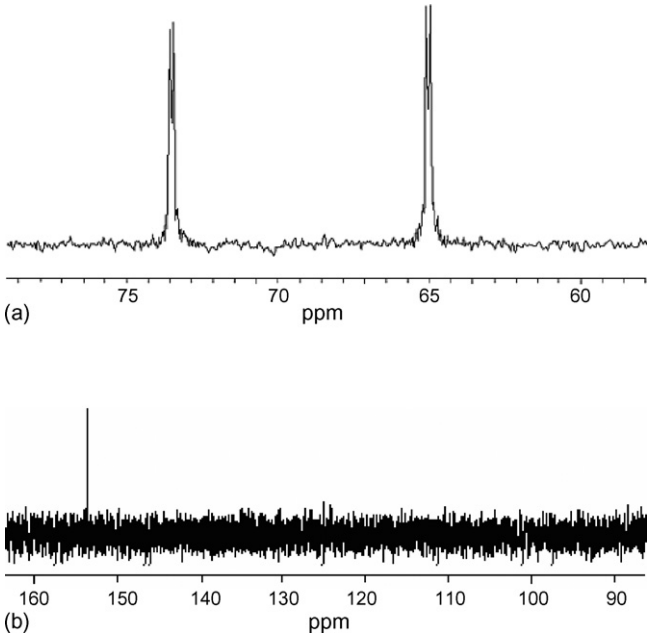

Fig. 1. ^{31}P NMR spectrum of (a) **1** and (b) **2** in CH_2Cl_2 (H_3PO_4/85%).

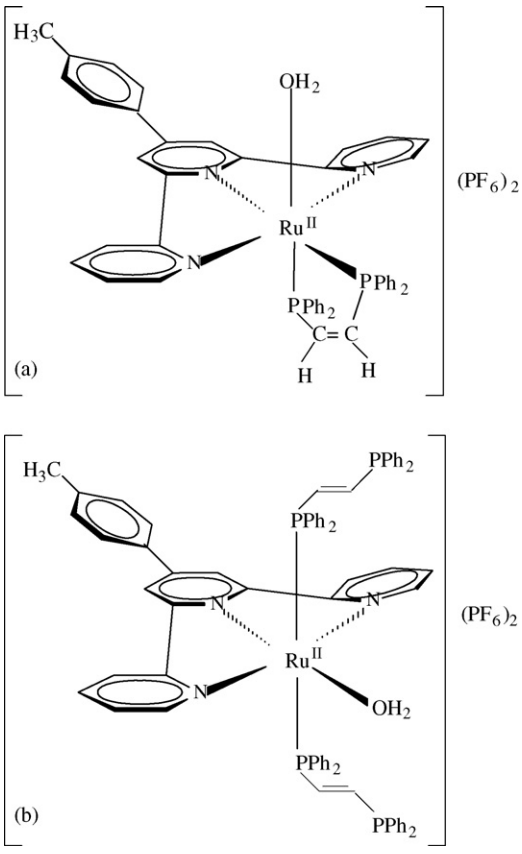

Fig. 2. Structure of: (a) [Ru(*cis*-L)(totpy)(H_2O)](PF_6)$_2$ (**1**) and (b) [Ru(*trans*-L)$_2$(totpy)(H_2O)](PF_6)$_2$ (**2**) (L = 1,2-bis(diphenylphosphino)ethylene; totpy = 4′-(4-tolyl)-2,2′:6′,2″-terpyridine).

3.4. Electrochemistry

The cyclic voltammogram data obtained for the complexes are summarized in Table 2. The chloro complexes exhibit reversible one-electron oxidations; the Ru(III/II) redox couple is +1.21 V (versus Ag/AgCl) for the *cis*-complex and +1.03 V for the *trans*-complex. This decrease in potential ongoing from the *cis*- to the *trans*-complex is well established in Ru(II) chemistry [13]. The eletronic nature of the ligands are very similar, but the peculiar oxidation potentials are probably a result of the different environments created by the two phosphine ligands in the *trans*-complex. The corresponding aqua complexes show two reversible redox waves corresponding to the Ru(III/II) and Ru(IV/III) redox couples (+1.22/+1.54 V and +1.08/+1.32 V versus Ag/AgCl, for the *cis*- and *trans*-complex, respectively, in CH_2Cl_2). Fig. 3a shows the cyclic voltammogram and b

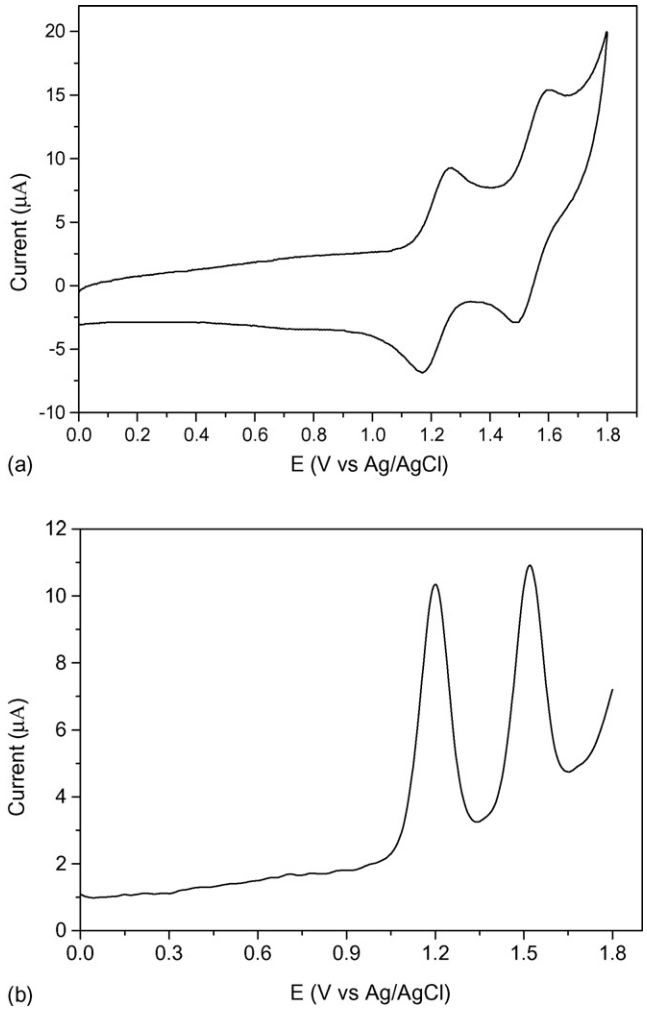

Fig. 3. (a) Cyclic voltammogram and (b) differential pulse voltammogram of 1.0×10^{-3} mol L^{-1} [Ru(*cis*-L)(totpy)(H_2O)](PF_6)$_2$ (**1**) (L = 1,2-bis(diphenylphosphino)ethylene) in CH_2Cl_2 + 0.1 mol L^{-1} TBAP, glassy carbon working electrode; (a) ν = 100 mV s^{-1}; (b) 10 mV s^{-1}.

Table 2
Electrochemical and spectral data for the complexes

Complexes	$E_{1/2}$ (V)		λ_{max} (nm) ($\varepsilon_{max} \times 10^3$, mol^{-1} L cm^{-1})
	Ru(III/II)	Ru(IV/III)	
[$RuCl_3$(totpy)]	+0.05[a]	–	226 (17), 285 (16), 310 (13), 406 (4.7)[b]
[Ru(*cis*-L)(totpy)Cl]Cl	+1.21[c]	–	290 (32), 319 (31), 432 (7.5)[d]
[Ru(*trans*-L)$_2$(totpy)Cl](PF_6)	+1.03[c]	–	290 (43), 308 (36), 487 (6.8)[d]
[Ru(*cis*-L)(totpy)(H_2O)](PF_6)$_2$ (**1**)	+1.22, +0.99	+1.54[c], +1.11[e]	290 (25), 320 (24), 418 (7.0)[d]
[Ru(*trans*-L)$_2$(totpy)(H_2O)](PF_6)$_2$ (**2**)	+1.08, +0.87	+1.32[c], +1.05[e]	289 (42), 306 (46), 475 (8.4)[d]

[a] MeCN + 0.1 mol L^{-1} TBAP; glassy carbon working electrode; ν = 100 mV s^{-1}.
[b] CH_3CN.
[c] CH_2Cl_2 + 0.1 mol L^{-1}; glassy carbon working electrode; ν = 100 mV s^{-1}.
[d] CH_2Cl_2.
[e] 7:3 phosphate buffer (μ = 0.20 mol L^{-1}):*tert*-butyl alcohol solution, pH 6.8.

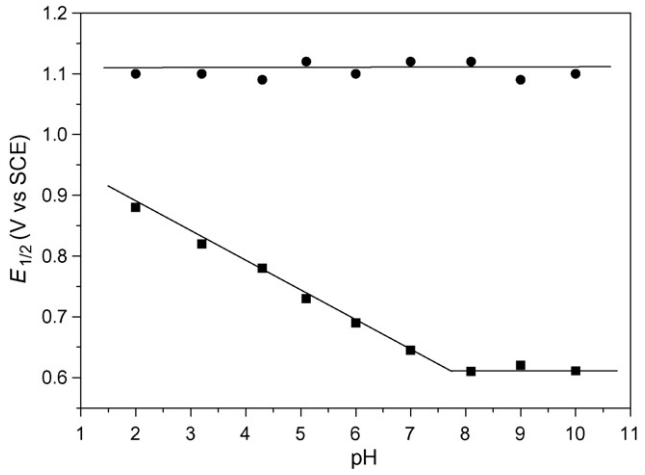

Fig. 4. Plots of $E_{1/2}$ vs. pH for the Ru(III/II) (■) and Ru(IV/III) (●) redox couples of [Ru(*cis*-L)(totpy)(H_2O)](PF_6)$_2$ (**1**); glassy carbon working electrode.

shows the pulse differential voltammogram of the *cis*-complex. In general, the cyclic voltammograms of the complexes in aqueous solutions have less well-behaved redox waves than those obtained in methylene chloride. The redox potentials of **2** are also less anodic, reflecting the electron-donation effect of the two phosphine ligands. The potentials observed in methylene chloride are higher than those obtained in aqueous solution (Table 2), and the separation between the two couples (mV) is larger than in water. This behaviour can be due to a very slow deprotonation kinetics of the first oxidized species; the deprotonation of the aqua ligand to form Ru^{III}–OH is facilitated in aqueous solution, but not in methylene chloride (a low protic and little polar solvent). These data are practically the same as those reported for the analogous [Ru(tpy)(dppene)(H_2O)](PF_6)$_2$ (tpy = 2,2′:6′,2″-terpyridine; dppene = *cis*-1,2-bis(diphenylphosphino)ethylene) complex [12]: $E_{1/2}$ = +1.17 and +1.53 V. These values are close to those found for **1** ($E_{1/2}$ = +1.22 and +1.54 V), indicating that the bulky donating tolyl group in position 4′ of the terpyridine ligand practically has no influence on the redox behaviour of the complex.

3.5. $E_{1/2}$ versus pH of the aqua complex *1*

The Pourbaix diagram for aqua complex **1** reveals two different pH regimes for the Ru(III/II) and Ru(IV/III) redox couple. The potentials of the Ru(III/II) redox couples vary with the pH of the solution, resulting in the $E_{1/2}$ versus pH variations shown in Fig. 4. Within the 8.0 > pH > 2.0 region, the potentials form a straight line with slope −0.051, which is very close to the Nernstian prediction of −0.059 V/pH unit, indicative of a one-electron oxidation accompanied by the dissociation of one proton (Scheme 1). At pH > 8.0, the potentials become pH-independent indicating that $[Ru^{II}(cis\text{-L})(totpy)(OH)]^+$ is the dominant species in this region (Scheme 2) [8,28].

$$[Ru^{II}(cis\text{-L})(totpy)(OH_2)]^{2+} \underset{+e^-,+H^+}{\overset{-e^-,-H^+}{\rightleftharpoons}} [Ru^{III}(cis\text{-L})(totpy)(OH)]^{2+}$$

Scheme 1.

$$[Ru^{II}(cis\text{-L})(totpy)(OH)]^{+} \underset{+e^-}{\overset{-e^-}{\rightleftharpoons}} [Ru^{III}(cis\text{-L})(totpy)(OH)]^{2+}$$

Scheme 2.

$$[Ru^{III}(cis\text{-L})(totpy)(O)]^{+} \underset{+e^-}{\overset{-e^-}{\rightleftharpoons}} [Ru^{IV}(cis\text{-L})(totpy)(O)]^{2+}$$

Scheme 3.

The Ru(IV/III) redox couple is not pH-dependent. Therefore, the species present at any pH is Ru(III)–O^+ and the determinant step does not involve protons [8,28] (Scheme 3).

3.6. Electrocatalysis

3.6.1. Electrocatalytic oxidations of organic substrates in homogeneous solution

The catalytic activities of **1** and **2** toward a variety of organic substrates (benzyl alcohol, cyclohexanol, cyclohexene, 1-pentanol, 1,2-butanediol, and 1,4-butanediol) were studied in 7:3 phosphate buffer:*tert*-butyl alcohol solutions, pH 6.8; *tert*-butyl alcohol was added to improve the solubility of the aqua complexes and substrates. Mixed solvent systems have been used by other groups in similar experiments, with no adverse effects [10,15].

In the presence of excess benzyl alcohol (50 times), the cyclic voltammograms of the complexes show great enhancement in the oxidation current peaks and decrease in the reduction peaks reversal potential scans (Fig. 5) shows the process for **1**, which is typical of electrocatalysis [8]. For the quantitative evaluation of the electrocatalytic behaviour of **1**, the dependence of the current peak height on the concentration of benzyl alcohol and on the potential scan rate was studied [29]. The peak height is linearly dependent (Fig. 6, correlation coefficient = 0.996, plot intercept near zero) on the concentration of benzyl alcohol, indicating that the electrocatalysis is *pseudo-first-order* in this benzyl alcohol concentration range.

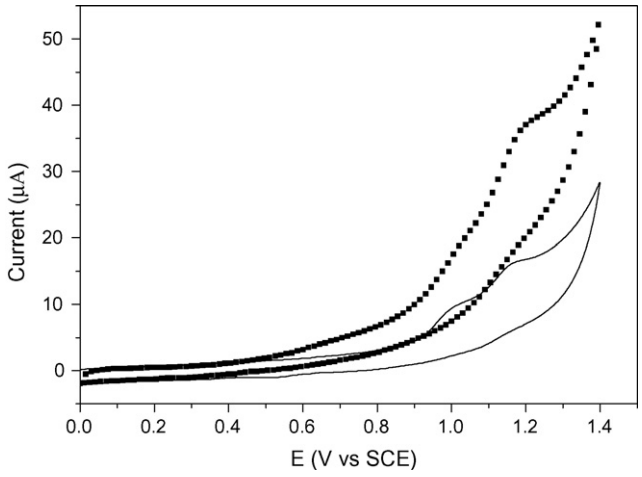

Fig. 5. Cyclic voltammograms of **1** (1.0 mmol L^{-1}) in the absence (—), and in the presence (···) of benzyl alcohol, in 7:3 phosphate buffer:*tert*-butyl alcohol solutions, pH 6.8; ν = 100 mV s^{-1}; [substrate] = 50 mmol L^{-1}.

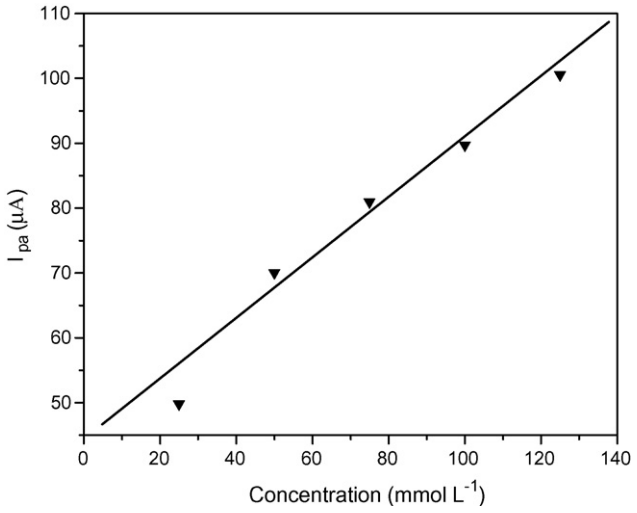

Fig. 6. Plot of the oxidation peak currents of **1** against benzyl alcohol concentrations; in 7:3 phosphate buffer:*tert*-butyl alcohol solutions, pH 6.8; $\nu = 100\,mV\,s^{-1}$.

Bulky electrolyses were conducted at controlled potentials of +1.18 V (versus SCE) for complex **1**, and +1.10 V (versus SCE) for complex **2**. The reactivities of the different substrates with respect to electro-oxidation could be obtained by the relation between product yields and electrolysis time. In this case, it is assumed that the rate-determining step is substrate oxidation, considering that the heterogeneous re-oxidation rates of the complexes at the electrode surface are much higher than the chemical reaction rates. Results of the electrocatalytic oxidations are summarized in Table 3. The relationship current efficiency by time unit gives the following reactivity order for the electro-oxidation for **1**: benzyl alcohol > cyclohexanol > cyclohexene > 1,4-butanediol > 1,2-butanediol > 1-pentanol; and for **2**: benzyl alcohol > cyclohexanol > cyclohexene > 1,4-butanediol > 1-pentanol > 1,2-butanediol. The proposed mechanism for oxidations using ruthenium oxo complexes suggests the formation of an electron-deficient carbon in the transition state [30]. A substituent group can decrease the reaction activation energy, inducing delocalization of the positive charge via hyperconjugation, inductive, or resonance effects. The secondary alcohol and the primary aromatic alcohol are more reactive than cyclohexene. In the case of benzyl alcohol, the resonance effect in its aromatic ring is responsible by positive charge delocalization. In cyclohexene, the allylic carbocation formed at C-3 before the attack of the water molecule (SN_2 reaction) induces a stabilization by resonance with a conjugated unsaturation at the carbon ring. Nevertheless, because cyclohexene has fewer canonic structures than benzyl alcohol, the lower positive charge delocalization decreases the reactivity. A higher reactivity of the primary alcohol when compared to that of the secondary one was also observed in homogeneous catalysis [8]. Benzaldehyde and benzoic acid are the products generated from the oxidation of benzyl alcohol; when the phosphine complex is used, though, benzaldehyde is the only oxidation product.

The following generalization is possible for the systems studied in this work: secondary alcohols and primary aromatic alcohols are more reactive than olefins, the latter being more reactive than primary aliphatic alcohols and diols. Complex **2**, which has the lowest Ru(IV/III) couple redox potential, is less reactive than complex **1**, indicating a direct relation between redox potential and reactivity of the complexes: the higher the $E_{1/2}$, the higher the reactivity [7].

*3.6.2. Electrocatalysis of organic substrates with carbon paste electrode containing complexes **1** and **2** (CPE)*

The cyclic voltammetric behaviour of CPE, in presence of organic substrates, in 7:3 phosphate buffer:*tert*-butyl alcohol solutions, pH 6.8, shows pronounced enhancement in the anodic currents corresponding to the Ru(IV/III) couple. There were no reduction peaks upon reversal scan direction, which is typical of electrocatalytic processes. The reactivity order is similar to that observed in homogeneous catalysis. The higher reactivity of benzyl alcohol can be due to its higher permeability into the active surface of the carbon paste electrode.

The dependence of the peak height on the bulk concentration of benzyl alcohol and on the potential scan rate indicates that the electrocatalysis is *pseudo-first-order* in the studied benzyl alcohol concentration range, as observed in homogeneous catalysis. The anodic peak currents change linearly with the square root of the scan rate (Fig. 7), which is typical of surface electrocatalysis with the catalyst confined to the electrode surface under diffusion rate control of the substrates from solution. This same

Table 3
Electrocatalytic oxidations of organic substrates by [Ru(*cis*-L)(totpy)(H_2O)](PF_6)$_2$ (**1**) and [Ru(*trans*-L)$_2$(totpy)(H_2O)](PF_6)$_2$ (**2**)[a]

Substrate[b]	Oxidative coulombs passed		Reaction time (min)		Products	Yields (%)	
	1	**2**	**1**	**2**		**1**	**2**
Benzyl alcohol	324.8	319.7	78	162	Benzaldehyde	64[c]	66[c]
Cyclohexene	580.0	520.6	126	144	2-Cyclohexen-1-one	59[d]	42[d]
1-Pentanol	196.8	232.1	252	300	1-Pentanal	33[c]	31[c]
Cyclohexanol	295.7	302.5	72	138	Cyclohexanone	48[c]	34[c]
1,2-Butanediol	348.1	315.2	258	390	1-Hydroxy-2-butanone	62[c]	55[c]
1,4-Butanediol	289.5	299.3	240	294	γ-Butyrolactone	56[c]	47[c]

[a] 7:3 phosphate buffer:*tert*-butyl alcohol solution, pH 6.8. Catalyst concentration 1.0 mmol L^{-1}. Applied potential (vs. SCE): +1.18 V for **1**, +1.10 V for **2**.
[b] Substrate concentration 50.0 mmol L^{-1}.
[c] Based on total coulombs passed taking into account a 2 e/mol reaction.
[d] Based on total coulombs passed taking into account a 4 e/mol reaction.

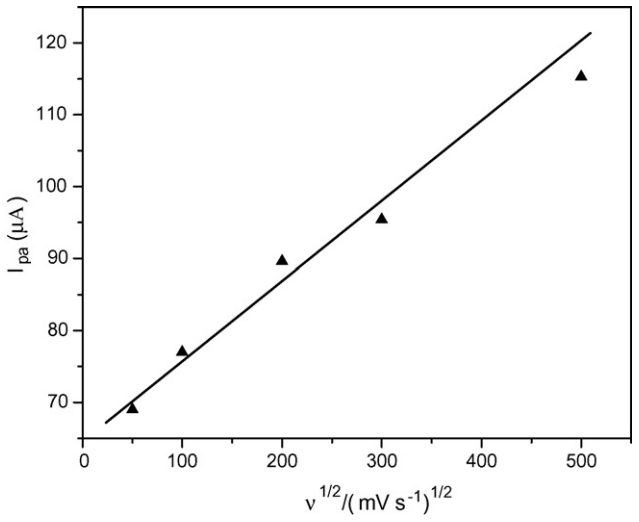

Fig. 7. Plot of the oxidation peak currents of CPE against the square root of the scan rates of **1** in the presence benzyl alcohol (50 mmol L^{-1}), several scan rates, in 7:3 phosphate buffer:*tert*-butyl alcohol solutions, pH 6.8.

behaviour was also observed in heteregenous catalysis by using aqua polypyridyl complexes [8].

4. Conclusions

The same products were obtained in the oxidation of various substrates in the presence of complexes **1** and **2**, but with different yields. Best results were obtained with the complex [Ru(*cis*-L)(totpy)(H_2O)](PF_6)$_2$ (**1**), which has a higher redox potential than the complex [Ru(*trans*-L)$_2$(totpy)(H_2O)](PF_6) (**2**). There is a direct relation between redox potential and reactivity of the complexes: the higher the $E_{1/2}$, the higher the reactivity.

Electrocatalysis of organic substrates with carbon paste electrodes containing complexes **1** or **2** (CPE) presents some advantages: the preparation of the carbon paste electrode is simple and straight forward, and the characteristics of the mediators are maintained upon their transfer from the solution to the immobilized state.

Our results showed the electrocatalytic potential of complexes **1** and **2** in the electro-oxidation of alcohols and olefins. These complexes can also be useful in the oxidation of other functional groups.

Acknowledgement

The authors thank Fundação de Amparo a Pesquisa do Estado de São Paulo (FAPESP) for financial support.

References

[1] (a) M. Sykora, J.C. Yong, T.J. Meyer, J. Phys. Chem. B 109 (2005) 1499–1504;
(b) J.A. Moss, J.C. Yong, J.M. Stipkala, X.G. Wen, C.A. Bignozzi, G.J. Meyer, T.J. Meyer, Inorg. Chem. 43 (2004) 1784–1792.
[2] E. Eskelinen, M. Haukka, T.J.J. Kinnunen, T.A. Pakkanen, J. Electroanal. Chem. 556 (2003) 103–108.
[3] C.A. Bessel, P. Aggonwal, A.C. Marschilok, K.J. Takeuchi, Chem. Rev. 101 (2001) 1031–1066.
[4] M. Navarro, M.N. Collomb, A. Deronzier, J. Electroanal. Chem. 520 (2002) 150–156.
[5] M. Rodríguez, I. Romero, C. Senz, A. Llobet, A. Deronzier, Electrochim. Acta 48 (2003) 1047–1054.
[6] T.J. Meyer, H.V. Huynh, Inorg. Chem. 42 (2003) 8140–8160.
[7] (a) M. Navarro, W.F. De Giovani, J.R. Romero, J. Mol. Catal. A: Chem. 135 (1998) 249–256;
(b) M. Navarro, W.F. De Giovani, J.R. Romero, Synth. Commun. 20 (1990) 399–406.
[8] E.C. Lima, P.G. Fenga, J.R. Romero, W.F. De Giovani, Polyhedron 17 (1998) 313–318.
[9] J.M. Madurro, G. Chiericato Jr., W.F. De Giovani, J.R. Romero, Tetrahedron Lett. 29 (1988) 765–768.
[10] S.B. Billings, M.T. Mock, K. Wiacek, M.B. Turner, W.S. Kassel, K.J. Takeuchi, A.L. Rheingold, W.J. Boyko, C.A. Bessel, Inorg. Chim. Acta 355 (2003) 103–115.
[11] (a) C. Chamchoumis, P.G. Potvin, Chem. Res. (S) (1998) 180–181;
(b) E.C. Constable, P. Harverson, D.R. Smith, L.A. Whall, Tetrahedron 50 (1994) 7799–7806.
[12] (a) V.J. Catalano, R.A. Heck, A. Öhman, M.G. Hill, Polyhedron 19 (2000) 1049–1055;
(b) V.J. Catalano, T.J. Craig, Inorg. Chem. 42 (2003) 321–334.
[13] M.O. Santiago, C.L.D. Filho, I.S. Moreira, R.M. Carlos, S.L. Queiroz, A.A. Batista, Polyhedron 22 (2003) 3205–3211.
[14] A. Dovletoglou, S.A. Adeyemi, T.J. Meyer, Inorg. Chem. 35 (1996) 4120–4127.
[15] V.J. Catalano, R. Kurtaran, R.A. Heck, A. Öhman, M.G. Hill, Inorg. Chim. Acta 286 (1999) 181–188.
[16] A. Llobet, Inorg. Chim. Acta 221 (1994) 125–131.
[17] X. Sala, A. Poater, I. Romero, M. Rodríguez, A. Llobet, X. Solans, T. Parella, T.M. Santos, Eur. J. Inorg. Chem. (2004) 612–618.
[18] K. Araki, H. Winnischofer, H.E.B. Viana, M.M. Toyama, F.M. Engelmann, I. Mayer, A.L.B. Formiga, H.E. Toma, J. Electroanal. Chem. 562 (2004) 145–152.
[19] J.G. Muller, J.H. Acquaye, K.J. Takeuchi, Inorg. Chem. 31 (1992) 4552–4557.
[20] S.A. Trammell, J.C. Wimbish, F. Odobel, L.A. Gallagher, P.M. Narula, T.J. Meyer, J. Am. Chem. Soc. 120 (1998) 13248–13249.
[21] J.P. Santos, M.E.D. Zaniquelli, C. Batalini, W.F. De Giovani, J. Phys. Chem. B 105 (2001) 1780–1785.
[22] J.P. Santos, M.E.D. Zaniquelli, C. Batalini, W.F. De Giovani, Thin Solid Films 349 (1999) 238–243.
[23] F. Tobalina, F. Pariente, L. Hernández, H.D. Abrunã, E. Lorenzo, Anal. Chim. Acta 395 (1999) 17–26.
[24] J.L. Chen, L.Y. Zhang, Z.N. Chen, L.B. Gao, M. Abe, Y. Sasaki, Inorg. Chem. 43 (2004) 1481–1490.
[25] R. Zhang, C.L. Kee, W.K. Leong, Y.K. Yan, J. Organomet. Chem. 689 (2004) 2837–2844.
[26] L.S. Luh, L.K. Liu, Inorg. Chim. Acta 206 (1993) 89–95.
[27] A.S. Silva, R.M. Carlos, A.J. Camargo, C.M.C. Picchi, R.H.A. Santos, B.R. McGarvey, D.W. Franco, Inorg. Chim. Acta 357 (2004) 3147–3154.
[28] K.J. Takeuchi, M.S. Thompson, D.W. Pipes, T.J. Meyer, Inorg. Chem. 23 (1984) 1845–1851.
[29] W. Kutner, J.A. Gilbert, A. Tomaszewski, T.J. Meyer, R.W. Murray, J. Electroanal. Chem. 205 (1986) 185–207.
[30] (a) M.S. Thompson, T.J. Meyer, J. Am. Chem. Soc. 104 (1982) 4106–4115;
(b) M.S. Thompson, T.J. Meyer, J. Am. Chem. Soc. 104 (1982) 5070–5076.